Diffusion of HDO in Pure and Acid-Doped Ice Films

Susan P. Oxley, Caitlin M. Zahn, and Christopher J. Pursell*

Department of Chemistry, Trinity University, One Trinity Place, San Antonio, Texas 78212-7200

Received: April 12, 2006; In Final Form: July 25, 2006

In these experiments, a few bilayers of D_2O were vapor-deposited on a pure crystalline H_2O ice film or an ice film doped with a small amount of HCl. Upon deposition, H/D isotopic exchange quickly converted the D_2O layer into an HDO-rich mixture layer. Infrared absorption spectroscopy followed the changes of the HDO from the initial HDO mixture layer to HDO isolated in the H_2O ice film. This was possible because isolated HDO in H_2O ice has a unique, sharp peak in the O−D stretch region that can be distinguished from the broad peak due to the initial HDO mixture layer. The absorbance of isolated HDO displayed first-order kinetics and was attributed to diffusion of HDO from the HDO-rich mixture layer into the underlying H_2O ice film. While negligible diffusion was observed for pure ice films and for ice films with HCl concentrations up to 1×10^{-4} mole fraction, diffusion of HDO occurred for higher concentrations of $(2-20) \times 10^{-4}$ mole fraction HCl with a concentration-independent rate constant. The diffusion under these conditions followed Arrhenius behavior for $T = 135-145$ K yielding $E_a = 25 \pm 5$ kJ/mol. The mechanism for the HDO diffusion involves either (i) molecular self-diffusion or (ii) long-range H/D diffusion by a series of multiple proton hop and orientational turn steps. While these spectroscopic results compare favorably with recent studies of molecular self-diffusion in low-temperature ice films, the diffusion results from all the ice film studies at low temperatures (ca. $T < 170$ K) differ from earlier bulk ice studies at higher temperatures (ca. $T > 220$ K). A comparison and discussion of the various diffusion studies are included in this report.

Introduction

The diffusion of water molecules in ice was studied in the past by several research groups. Older results were conveniently compiled by Hobbs,[1] while more recent studies were reviewed by Petrenko and Whitworth.[2] Because the diffusion coefficient is very small, all the older studies were performed at modestly low temperatures between ~238−271 K. These studies (i) used the isotopic probes $H_2{}^{18}O$, D_2O, and T_2O as tracers to follow the diffusion process, (ii) included bulk ice samples of polycrystalline ice, artificially grown single-crystal ice, and naturally grown single-crystal ice, and (iii) examined diffusion for different crystallographic orientations. Microtome sectioning of the bulk ice into very thin layers followed by scintillation or mass spectrometric detection was used to measure the diffusion of the tracer species. Studies indicated that diffusion of water molecules in ice involves molecular self-diffusion of intact water molecules since the diffusion coefficients for D_2O and $H_2{}^{18}O$ were approximately identical.[1,2]

As an example of the earlier tracer studies, Ramseier studied T_2O diffusion into artificially and naturally grown ice from 243 to 268 K.[3] Diffusion perpendicular to the optical axis (*c* axis) was observed to be greater (ca. ~ 12%) than diffusion parallel to the *c* axis. This anisotropy was attributed to the geometry of the lattice structure. It was concluded that molecular self-diffusion in ice takes place by a vacancy mechanism. However, others argued that diffusion occurred by an interstitial mechanism.[4]

The mechanism for molecular self-diffusion in ice was examined by Hondoh's laboratory[5−7] for $T \sim 220-269$ K. Using X-ray topography the variation of the size of dislocation loops as a function of temperature was measured. The results indicated that the predominant point defects in ice are H_2O interstitials and not vacancies. Interstitials are H_2O molecules in ice that do not occupy regular crystal lattice sites, while vacancies are unoccupied crystal lattice sites. Hondoh's research group also determined the diffusion coefficient of the H_2O interstitials, along with their equilibrium concentration. The energy of activation was determined to be the sum of two components: the energy of formation of interstitials and the activation energy for motion. Because the total energy of activation was consistent with those energies from the tracer studies, it was concluded that the mechanism for self-diffusion of water molecules in ice involves interstitial diffusion, at least for the temperature range ~220−269 K. Recent molecular dynamic studies from Hondoh's group confirmed this conclusion.[8,9]

More recently the diffusion of water in ice was examined for thin vapor-deposited ice films at low temperatures (ca. $T \leq 170$ K). The results suggest that diffusion in low-temperature ice films differs from diffusion in bulk ice samples at higher temperatures.

George's research group[10−12] studied the diffusion of $H_2{}^{18}O$ and HDO into H_2O ice from 146 to 170 K using a laser-induced thermal desorption technique with mass spectrometric detection. Multilayer crystalline ice was grown epitaxially on a Ru(001) metal substrate. After deposition of a thin ice film, a tracer molecule ($H_2{}^{18}O$ or HDO) was adsorbed onto the surface. Diffusion of the tracer molecule from the surface into the thin ice film was detected by isothermally desorbing the ice multilayer with a laser pulse and then monitoring the water species with mass spectrometry. While the determined energy of activation is similar to the values from the earlier bulk ice

* To whom correspondence should be addressed.

10.1021/jp062270v CCC: $33.50
Published on Web 08/31/2006

studies, their diffusion coefficients are more than 10^3 times larger than the value obtained by extrapolation of the tracer data to 160 K.

More recently Kang's research group[13,14] examined both vertical water diffusion and H/D isotopic exchange on very thin ice films using Cs^+ reactive ion scattering (RIS) with mass spectrometric detection. For this diffusion study, very thin amorphous H_2O ice films were vapor-deposited on Ru(0001) between 100 and 140 K. A fractional coverage of D_2O was then added onto the ice film. Vertical diffusion of D_2O into the H_2O ice film and reverse migration of H_2O to the surface resulted in a change in the surface concentration. This study provided information directly at the ice surface with a depth resolution of 1 BL. A first-order rate constant and activation energy were determined for diffusion from the surface into the amorphous ice film. The activation energy is similar to the energy associated with the motion of interstitials mentioned above and suggests that the measured diffusion is due to an interstitial mechanism. Using the first-order rate constant and the assumption that the probing depth for molecular diffusion is one interlayer spacing, a diffusion coefficient was estimated. This estimated diffusion coefficient is more than 10^5 times larger than the value obtained by extrapolation of the tracer data to 140 K.

In this report, a spectroscopic study of the diffusion of HDO into pure and acid-doped ice films is presented. These experiments consisted of the vapor deposition of a few bilayers of D_2O on a pure crystalline H_2O ice film or an ice film doped with a small amount of HCl. Upon deposition, H/D isotopic exchange quickly converted the D_2O layer into an HDO mixture layer. The diffusion of HDO from the mixture layer into the underlying crystalline H_2O ice film was monitored using infrared absorption spectroscopy, which was possible because isolated HDO in H_2O ice has a unique, sharp peak that can be distinguished from the initial broad peak of the HDO mixture layer. Previously,[15] the observed spectral changes were attributed to H/D isotopic exchange of D_2O *occurring on* H_2O ice, which is now believed to be wrong. In particular, (i) the initial D_2O layer was not pure D_2O but an HDO isotopic mixture and (ii) the spectral change observed for the acid-doped ice films was not due to H/D exchange on the ice surface but to interdiffusion of HDO and H_2O between the isotopic mixture layer and the H_2O ice film. In this report additional data are presented concerning the acid and temperature dependence, along with an analysis that attributes the spectral changes to HDO diffusion into an H_2O ice film. The results compare favorably with the other studies of diffusion in low-temperature ice films but differ from the earlier bulk ice studies at higher temperatures. A discussion of these differences for the diffusion of water in ice films and in bulk ice samples is included in this report.

Experimental Methods

Concentration Study. The experimental setup for this system has been described in detail.[15,16] In brief, ice films were grown by vapor deposition onto an infrared transparent ZnSe window positioned at the end of a coldfinger contained in a closed-cycle liquid-He cryostat (Advanced Research Systems DE 202 expander). The temperature of the window was measured and regulated by a silicon diode sensor and a LakeShore 321 temperature controller. The pressure within the cryostat was maintained at $P < 10^{-6}$ Torr, as measured with a cold cathode gauge. The cryostat system, with KBr outer windows, was situated in the sample compartment of a purged Nicolet Magna 550 series FTIR spectrometer.

Vapor was introduced from a glass line (volume $\approx$ 2 L) into the cryostat through a needle valve and a 6-in. piece of stainless steel tubing directed at the ZnSe window. H_2O and HCl/H_2O vapors were introduced through a separate needle valve and inlet system than the D_2O vapor to prevent cross-contamination. Vapors were from pure water (Aldrich, reagent grade), aqueous solutions of HCl (dilutions of water and Aldrich 37 wt % HCl, 99.999%), and pure D_2O (Cambridge Isotope Laboratories, 99.96%). The partial vapor pressures of HCl and H_2O were determined from the equilibrium pressures above the aqueous acid solutions at either 0 °C or room temperature.[17] The concentrations of the HCl solutions were determined by titration with a NaOH solution standardized with KHP. The mole fraction of HCl in an ice film was determined according to condensation kinetics, as explained below in the Results.

Experiments were performed by first introducing H_2O or HCl/H_2O vapor at a rate of $\sim$0.5 mTorr/s onto the ZnSe window at 150 K. The thickness of the deposited crystalline ice layer was determined using the known conversion value of 0.163 Abs/μm of ice at 824 cm^{-1}, giving a thickness of 0.50 ± 0.02 μm.[18] The infrared spectrum of the ice films confirmed the polycrystalline nature of the ice. After the ice was annealed at 150 K for at least 20 min, the window was cooled to the temperature of interest. About 1−2 mTorr of D_2O was then introduced into the cryostat, leading to an absorbance of 1.5−3.5 mAbs at 2424 cm^{-1}. Previous interference studies from this laboratory gave a conversion value of 2.35 Abs/μm for the O−D stretching band at 2424 cm^{-1} for pure crystalline D_2O ice.[15] Using this value, it is estimated that approximately 6−15 Å or $\sim$2−5 bilayers (BL) of D_2O were deposited on the ice. Infrared spectra were collected as a function of time for at least 1 h. To clearly observe the resulting spectra, the spectrum of the underlying ice film was used as the background. In all cases, spectra were acquired by averaging 32 scans with a resolution of 4 cm^{-1} and an acquisition time of 39.5 s.

Temperature Study. The experimental setup for the temperature study was the same as that for the concentration study, except the cryostat was also equipped with a turbomolecular pump situated directly above the ZnSe window. The temperature range for these experiments was dictated by extraneous ice deposition below 135 K and ice loss by sublimation above 145 K. The minimal deposition or sublimation in this temperature range was taken into account by calibration of ice films without D_2O. This calibration resulted in a small adjustment ($\sim$10%) in the measured k values.

Experiments were performed by first introducing 20×10^{-4} mole fraction HCl vapor at a rate of $\sim$0.5 mTorr/s onto the ZnSe window at 150 K. The thickness of the deposited film was 0.50 ± 0.01 μm, based upon the same conversion as in the concentration study. The infrared spectrum of these acid-doped ice films indicated that the films appeared to be essentially pure crystalline ice. The ice was annealed at 150 K for at least 10 min and then cooled to the temperature of interest. The temperature was recorded and maintained to $\pm$0.1 K throughout the course of the experiment. Roughly 2−5 BL of D_2O were deposited on the ice, and infrared spectra were collected as a function of time for at least 2 h. To clearly observe the resulting spectra, the spectrum of the underlying ice film was used as the background. In all cases, spectra were acquired by averaging 32 scans with a resolution of 4 cm^{-1} and an acquisition time of 39.5 s.

Results

Figure 1 shows the change in the infrared absorption spectra of the O−D stretch region as a function of time when 2−5 BL of D_2O were deposited at 145 K on (a) a pure H_2O ice film and

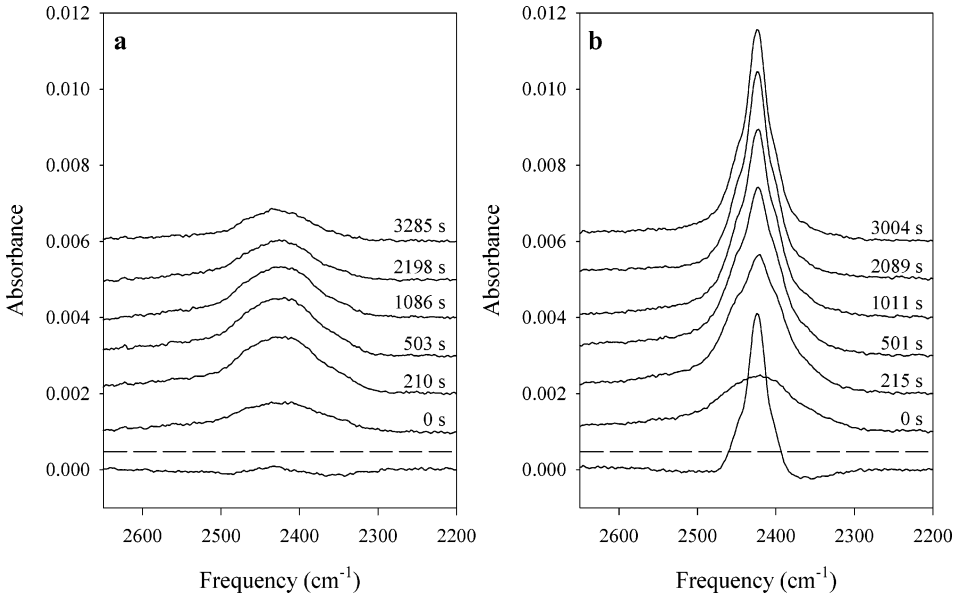

Figure 1. Infrared absorption spectra as a function of time for 2−5 BL of D_2O deposited at 145 K on (a) pure H_2O ice film, showing negligible spectral changes, and (b) 2×10^{-4} mole fraction HCl-doped H_2O ice film (ca. 1 HCl to 5000 H_2O molecules), indicating the appearance of isolated HDO in ice. The spectra situated below the dashed line are the subtraction of $t = 0$ from the $t = 3285$ and 3004 s spectra for pure ice and 2×10^{-4} mole fraction HCl-doped ice, respectively. For this particular data, approximately twice as much D_2O was deposited on the acid-doped ice film as on the pure ice film, as evidenced by the ∼2× absorbance at $t = 0$ s. D_2O deposition was complete after ∼200 s. The absorbance scales for (a) and (b) are the same, and the spectra are offset for clarity.

(b) an acid-doped H_2O ice film. On the pure ice film, the shape of the resulting broad peak did not appear to change appreciably during the time probed (ca. up to 2 h). However, when the H_2O ice film was doped with HCl (ca. 2×10^{-4} mole fraction HCl, or 1 molecule of HCl to 5000 H_2O molecules), the O−D stretch spectrum changed significantly as the band at 2424 cm^{-1} narrowed and increased in absorbance, indicative of HDO *isolated* in H_2O ice. It should be noted that well over 50 experiments have been performed on pure and acid-doped ice films, consistently yielding these results. The $t = 0$ s spectra in Figure 1 correspond to the first spectra acquired; since spectral acquisition takes a definite period of time (39.5 s), the $t = 0$ spectra correspond to the average of the first 39.5 s. The deposition of the D_2O layer was complete within the first 200 s of exposure.

Previously,[15] the results displayed in Figure 1 had been interpreted in terms of H/D isotopic exchange of D_2O *occurring on* the H_2O ice surface. Since the initial spectrum of D_2O on a pure ice film did not appear to change during the course of the experiment, it was concluded that no isotopic exchange occurred. This conclusion conflicted with the extensive and thorough work from Devlin's laboratory concerning isotopic exchange in ice.[2,19,20] Furthermore, since isotopic exchange involves a proton hop step, it was suggested that there are few active protons on the pure ice surface, thus the need for doping the ice film with acid in order for exchange to occur. It was concluded[15] that the results were unique and differed from Devlin's work because isotopic exchange was being examined *on* the ice surface as opposed to *in* ice. However, the previous interpretation of these results in terms of H/D isotopic exchange now appears to be wrong. In particular and as demonstrated below, (i) the initial D_2O layer was not pure D_2O but an HDO isotopic mixture and (ii) the spectral change observed for the acid-doped ice films was not due to H/D exchange but to the diffusion of HDO into the H_2O ice film.

Concerning the initial D_2O, the 2−5 BL D_2O layer is not a pure layer but an isotopic mixture. According to the recent work from Kang's laboratory,[13,14] vertical diffusion and H/D isotopic exchange occur very quickly at the surface (ca. 1−5 BL) of ice films from 90 to 140 K. Therefore, upon vapor deposition of D_2O on an H_2O ice film over the temperature range 135−145 K, short-range vertical diffusion and H/D isotopic exchange quickly convert the thin D_2O layer into an isotopic HDO mixture layer. George's group observed the same type of rapid isotopic exchange of D_2O on an H_2O film at 120 K.[11]

To confirm that H/D isotopic exchange occurred and to determine the composition of the resulting HDO mixture layer, various D_2O ice spectra were collected for comparative purposes. Figure 2a shows the spectrum for 2−5 BL of D_2O deposited on a pure H_2O ice film just after deposition at 145 K (ca. the $t = 210$ s spectrum from Figure 1a). This peak is broad (fwhm = 114 cm^{-1}) and featureless. An amorphous D_2O ice film at 80 K (Figure 2e) is broader and shifted to a higher frequency, while a crystalline D_2O ice film at 150 K (Figure 2d) shares a common maximum with the D_2O layer spectrum but has two pronounced shoulders. Thus, the initial D_2O layer is not "pure" amorphous or crystalline D_2O ice. Ice films prepared by mixing an ∼1:1 ratio of D_2O and H_2O in the vapor phase and then depositing at 80 K (cf. amorphous) and 150 K (cf. crystalline) are shown in Figure 2b and c, respectively. The vapors were mixed in the ∼2 L glass line where isotopic scrambling on the glass surface produced an equilibrium gas composition of 25% D_2O:50% HDO:25% H_2O. The amorphous ice spectrum is broader and shifted to a higher frequency, while the crystalline ice spectrum appears to match the spectrum of the initial D_2O layer. The crystalline ice-mixture spectrum also matches the published ice spectrum of Haas and Horning for this same composition.[21]

Thus, the spectrum observed just after the deposition of 2−5 BL D_2O layer on crystalline H_2O ice films, for both pure and acid-doped ice at 145 K (Figure 2a), closely resembles the spectrum of the crystalline ice mixture of Figure 2b. *The initial D_2O layer is therefore not a pure D_2O ice layer but is actually an isotopically mixed layer of D_2O, HDO, and H_2O.* On the basis of a comparison of the spectra in Figure 2 (parts a and b), the composition of the layer is estimated to be 25% D_2O:50%

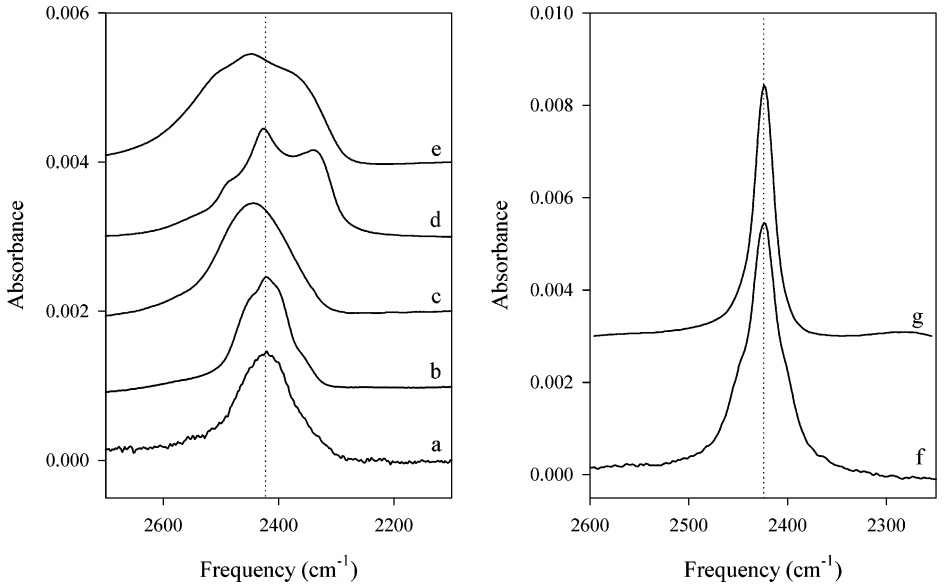

Figure 2. Infrared absorption spectra of the O−D stretch region for (a) 2−5 BL of D_2O on pure crystalline H_2O ice film just after deposition at 145 K, (b) crystalline ice film from deposition of ∼1:1 gas mixture of D_2O and H_2O at 150 K (film composition is 25% D_2O:50% HDO:25% H_2O), (c) amorphous ice film from deposition of ∼1:1 gas mixture of D_2O and H_2O at 80 K (film composition is 25% D_2O:50% HDO:25% H_2O), (d) pure crystalline D_2O ice film at 150 K, (e) pure amorphous D_2O ice film at 80 K, (f) 2−5 BL of D_2O on 2×10^{-4} mole fraction HCl-doped ice film 1 h after deposition at 145 K, and (g) isolated HDO in crystalline H_2O ice film at 150 K. Spectra have been offset for clarity. Reference spectra (b−e, g) have been scaled to the same absorbance as the unscaled reaction spectra (a, f).

HDO:25% H_2O. The thickness is estimated to be 4−10 BL, or two times 2−5 BL of D_2O. This estimate is consistent with a study from George's research group, where rapid and complete H/D exchange was observed that converted 1.5 BL of D_2O on a thin H_2O ice film at 120 K into a localized 3 BL HDO adlayer.[11]

If we return to Figure 1, while no spectroscopic changes were observed for the pure ice films, significant changes occurred for the acid-doped ice films. *These spectroscopic changes are attributed to the interdiffusion (or isotopic mixing) of HDO from the HDO-rich mixture layer into the underlying H_2O ice film and of H_2O from the film into the HDO-rich mixture layer*. The sharp peak at 2424 cm^{-1} that grows in with time is due to the formation of HDO *isolated* in the H_2O ice film, which can easily be distinguished from the initial spectrum of the HDO mixture layer. The resulting spectrum (Figure 2f) is significantly sharper (fwhm = 26 cm^{-1}) than the spectrum for the HDO mixture layer (Figure 2a) and compares favorably with the spectrum of HDO isolated in bulk crystalline ice (Figure 2g). The reference spectrum of isolated HDO was obtained by depositing an H_2O ice film that possessed a very small amount of HDO. This was accomplished in the following way: D_2O vapors were introduced into the glass line and removed; H_2O vapors were then introduced and H/D exchange occurred on the glass line producing a very small amount of HDO. The resulting H_2O vapors with a very small amount of HDO (ca. < 1%) were then deposited as an ice film. The resulting spectrum of isolated HDO in crystalline H_2O ice (Figure 2g) agrees with that reported by Devlin.[19]

The present spectroscopic results can be explained by the following expressions:

$$D_2O + H_2O \leftrightarrow (HDO)_2 \quad (1)$$

$$(HDO)_2 \rightarrow 2HDO\ (\textit{isolated}) \quad (2)$$

Step 1 represents the isotopic exchange equilibrium that is quickly established on the ice films, both pure and acid-doped, giving rise to the initial isotopic mixture layer (see Figure 2a).

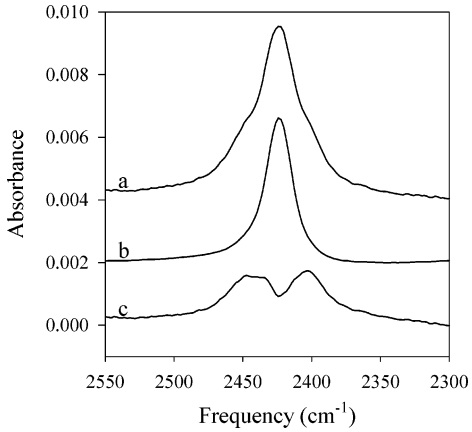

Figure 3. Infrared absorption spectra of the O−D stretch region at 145 K for (a) 2−5 BL of D_2O on 2×10^{-4} mole fraction HCl-doped ice film after 1 h, (b) isolated HDO in H_2O ice film, and (c) spectral subtraction (a) − (b), revealing the spectrum for $(HDO)_2$. Spectra are offset for clarity.

This fast preequilibrium step maintains a steady-state amount of the $(HDO)_2$ species. Step 2 represents the slower diffusion of HDO into the underlying ice film.

According to step 1, the $(HDO)_2$ species should be present in the initial mixture spectrum and should slowly decrease with time. On the basis of the relative amount of the isotopes in the initial mixture (ca. 25% D_2O:50% HDO:25% H_2O), 50% of the HDO should exist as the $(HDO)_2$ nearest neighbor, which Devlin identified in his studies.[19,20,22] To observe this species, an isolated HDO spectrum can be subtracted from the reaction spectrum, as shown in Figure 3. The subtraction yields two peaks at 2447 and 2403 cm^{-1}, in agreement with the $(HDO)_2$ spectrum reported by Devlin and co-workers.[22] To obtain this $(HDO)_2$ spectrum, it was assumed that 85% of the absorbance at 2424 cm^{-1} could be attributed to HDO. The HDO spectrum was then scaled accordingly, and the two spectra were subtracted with a subtraction factor of 1. This method is similar to that employed by Devlin and co-workers to isolate the $(HDO)_2$ spectrum.[22]

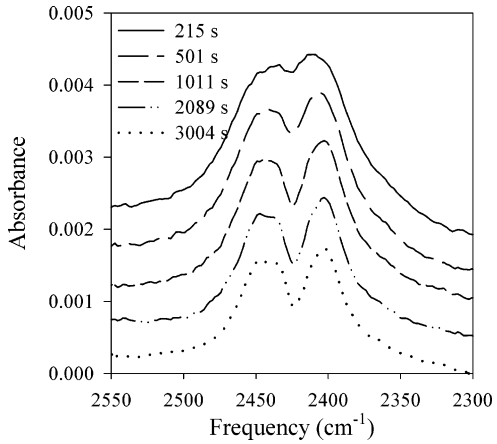

Figure 4. Infrared absorption spectra of $(HDO)_2$ as a function of time for 2−5 BL D_2O on 2×10^{-4} mole fraction HCl-doped ice at 145 K. Normalized isolated HDO spectra (Figure 3b) were subtracted from raw absorption spectra (Figure 1b) as described in the text. Spectra are offset for clarity.

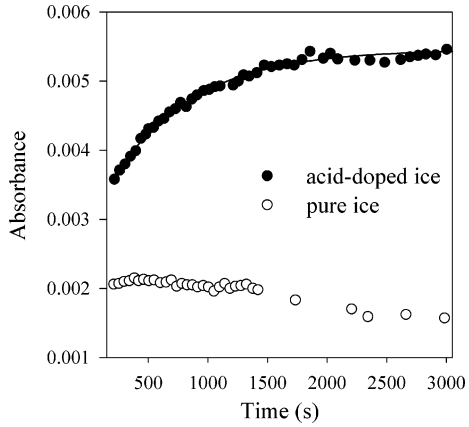

Figure 5. Absorbance at 2424 cm^{-1} as a function of time for an HDO mixture layer (4−10 BL) at 145 K on (○) pure H_2O ice film and (●) 2×10^{-4} mole fraction HCl-doped ice film. The solid line corresponds to a first-order fit (see eq 3). The data in this figure correspond to the spectra in Figure 1. A small amount of sublimation is observed for this pure ice sample as evidenced by the slight negative slope of the data after ∼1500 s (see text).

The evolution of the $(HDO)_2$ peak with time is shown in Figure 4. These spectra were obtained by subtracting an appropriately scaled isolated HDO spectrum from each spectrum in Figure 1b. The isolated HDO scaling factor was determined from the longest time spectrum ($t = 3004$ s) and the measured first-order rate constant (see below). The $(HDO)_2$ spectrum slowly decreases with time, and the two peaks become more distinct. These results indicate that the $(HDO)_2$ forms very quickly and is then slowly depleted over time by diffusion of HDO into the underlying ice film, consistent with step 1 (the fast preequilibrium step) and step 2 (the slower diffusion step) above. Note that even though the diffusion is ∼99% complete at $t = 3004$ s, $(HDO)_2$ is still clearly present.

According to step 2, the slow formation of isolated HDO dominates the observed spectral changes (see Figure 1b). To quantitatively characterize these changes, the absorbance at 2424 cm^{-1} was measured as a function of time, an example of which is shown in Figure 5. The data presented correspond to the spectra in Figure 1 at 145 K. These data were fit to a single exponential, first-order expression of the following form:

$$\text{absorbance} = A(1 - e^{-kt}) + B \qquad (3)$$

The data for the acid-doped ice film (filled circles) fit well to the single exponential, indicating first-order behavior and yielding a first-order rate constant, k, associated with step 2 above. The recent vertical diffusion studies by Kang's laboratory[13] also produced first-order behavior. For the 2×10^{-4} mole fraction HCl data shown in Figure 5, $k = 1.5 \times 10^{-3}$ s^{-1} at 145 K. Since the initial deposition of D_2O occurred over the first 200 s, these data were not included in the kinetic fits and are not included in Figure 5.

The absorbance at 2424 cm^{-1} for the HDO mixture layer on pure ice is also presented in Figure 5 (open circles). It is virtually constant for the first 1500 s and then slowly decreases at longer times as a result of sublimation. This slight sublimation loss is the only evidence of the dynamic nature of the ice surface from our study. Assuming an equilibrium vapor pressure of 7×10^{-9} Torr at 145 K, the condensation rate should equal the sublimation rate, which is calculated to be 0.02−0.2 BL/min for H_2O ice and 0.007−0.04 BL/min for D_2O ice at this temperature.[23−25] This constant reconstruction of the ice surface is believed to occur to only 2−3 BL deep, according to a molecular dynamics study for $T = 180-210$ K.[26] It is possible that our results may be affected by this fast exchange at the surface, where the depth of reconstruction is perhaps 1−2 BL deep for the present experimental temperatures. For example, if net condensation of H_2O were occurring throughout the experiment, then the D_2O/HDO layer would become embedded in the ice film. This would lead to rapid H/D exchange and the formation of isolated HDO. However, this was not observed on the pure ice films. If the vapor pressure of D_2O in the cryostat is much less than 7×10^{-9} Torr, this would lead to net sublimation of D_2O from the surface. Calculations, using the larger sublimation rate, indicate that ∼2 BL of D_2O ice should sublime after 3000 s at this temperature, which agrees with the data in Figure 5 and with the estimate of the HDO mixture layer thickness. Therefore, concerning the dynamic nature of the ice surface, the spectroscopic data indicate only the very slow sublimation of D_2O from the surface of pure ice films. On acid-doped ice films, this sublimation would compete with the HDO diffusion, causing the measured rate constants to be slightly smaller. The amount of sublimation was therefore taken into account by calibration of the sublimation of pure ice films at the appropriate temperatures. This calibration resulted in a small adjustment (∼10%) in the measured k values.

Concerning the acid concentration study, the first-order rate constant was determined according to eq 3 for ice films with various concentrations of HCl. The rate constant displays an "off-on" behavior as a function of HCl concentration, as shown in Figure 6. At concentrations below 1×10^{-4} mole fraction, negligible diffusion was observed, while, at concentrations of 2×10^{-4} mole fraction and above, HDO diffusion occurred. Within experimental error, the rate constant is constant for $(2-20) \times 10^{-4}$ mole fraction HCl with an average value of $(1.5 \pm 0.5) \times 10^{-3}$ s^{-1} at 145 K (ca. the average for the data from Figure 6).

The acidic ice films were not created under equilibrium conditions but by the co-condensation of HCl and H_2O vapors onto a cold infrared window. Since diffusion of HCl at these temperatures is thought to be very slow, the HCl should be evenly distributed in the ice films and the composition should be controlled by condensation kinetics.[27] Accordingly, the mole fraction of HCl in the ice has been determined as

$$X_{HCl} = (P_{HCl}/P_{H2O})(\alpha_{HCl}/\alpha_{H2O})(M_{H_2O}/M_{HCl})^{1/2} \qquad (4)$$

For the experimental temperature range, it was estimated that

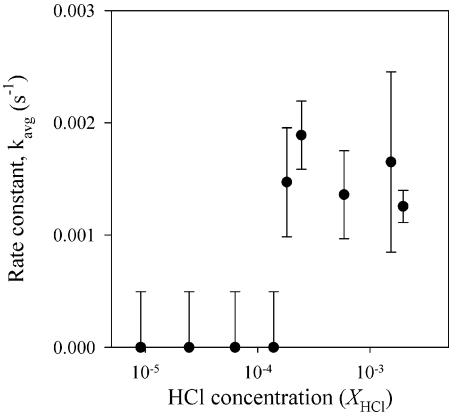

Figure 6. Averaged first-order rate constant as a function of mole fraction HCl in the ice film. Error bars for $k \neq 0$ points are ± one standard deviation from at least 3 measurements, while error bars for $k = 0$ points are the average of the nonzero standard deviation values.

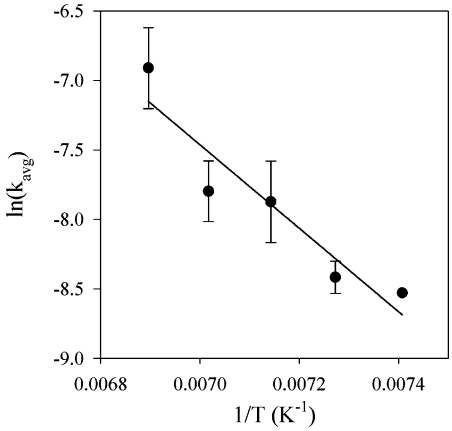

Figure 7. Arrhenius plot for the diffusion of an HDO mixture layer (4−10 BL) into 20×10^{-4} mole fraction HCl-doped ice film between 135 and 145 K. Circles represent data, and the line represents a linear fit of the data, yielding $E_a = 25 \pm 5$ kJ/mol. Error bars correspond to ± one standard deviation from at least four experiments. For $T = 135$ K the error bars are smaller than the size of the data point.

$\alpha_{HCl} \approx \alpha_{H_2O} = 0.8-1$, based upon measured mass accommodation coefficients.[23,28] The partial vapor pressures of HCl and H_2O were determined from the equilibrium pressures above the aqueous acid solutions. For the present experimental conditions, the HCl probably exists in ice in the form of an ionic solid solution, according to the HCl−H_2O temperature−composition phase diagram.[27]

The reason for the "off-on" behavior is unclear at this time. For the low concentrations up to 1×10^{-4} mole fraction (ca. 1 molecule of HCl to 10^4 molecules of H_2O), the HCl has probably been incorporated and ionized in the ice structure, forming protonic and Bjerrum *L*-defects but otherwise not significantly disrupting the ice lattice structure, at least in terms of increasing diffusion. For higher acid concentrations of 2×10^{-4} mole fraction and above, local microcrystals of the HCl hexahydrate may form within the solid ionic mixture. Hobbs has suggested that local clustering of impurities can occur in ice.[1] Formation of an HCl hydrate in the ice might be revealed by the infrared spectra. For both pure and acid-doped ice films, the spectra were qualitatively and quantitatively very similar due to the very low HCl concentrations and the spectroscopic detection limits. However, at the very highest acid concentration, a small broad absorption band between 1700 and 1900 cm^{-1} and a small sharp peak at 1635 cm^{-1} were detected, indicative of H_3O^+ due to the HCl hexahydrate.[29] A mixed ice−acid-hydrate solid would have an increased number of defects, especially dislocations and grain boundaries between the two microcrystalline solid regions.[27,30] Enhanced diffusion would then occur due to the increased number of defects. It is possible that once these microcrystalline regions are established, increasing the acid content of the ice films simply increased the relative size of the microcrystals but not necessarily the number of grain boundaries.

An additional explanation for the "off-on" behavior comes from very recent work by Kang's group.[31] They examined proton transfer and H/D diffusion in very thin ice films using Cs^+ reactive ion scattering and low-energy sputtering. Briefly, the results indicate that (1) protons can very quickly migrate from inside an "ice sandwich" to the surface, which is followed by a slower H/D diffusion by recurrence of a proton hop−molecular turn process, and (2) excess protons tend to collect at the surface where they become hydrated with increasing temperature and thereby buried just below the surface. For this study, this means that for the HCl-doped ice films the excess protons may not be homogeneously mixed throughout the ice film but may become concentrated near the surface. The "off-on" behavior may therefore be explained as follows. For the very lowest HCl concentrations, the protons may be more or less mixed in the ice. At the higher concentrations, the larger proton activity drives the protons to the surface. Once near the surface, the hydrated protons turn on the H/D diffusion, at which point the diffusion process is then controlled by the orientational turn step (see Discussion below).

George's group also observed concentration-independent processes in ice with acid dosing. The rate of D_2O desorption from and the rate of HDO diffusion into a thin film of ice was observed as a function of HCl and HNO_3 surface coverage.[24,32] The surface coverage of the acid was 0.3−5 BL for HCl and 0.5−3 BL for HNO_3. Over this range, the D_2O desorption rate and the HDO diffusion rate were independent of acid coverage. The changes in the measured rates relative to pure ice films were attributed to an increase in the number of protonic and Bjerrum *L*-defects in the case of HCl dosing and to the possible formation of acid hydrates for the HNO_3 dosing. No further explanation was given for the acid concentration independence.

Concerning the temperature studies, the first-order rate constant as a function of temperature was measured for 20×10^{-4} mole fraction HCl ice films. The *k* values were obtained according to eq 3 for $T = 135-145$ K. At least four experiments were performed at each temperature. The resulting first-order rate constants display Arrhenius behavior as shown in Figure 7 producing an activation energy $E_a = 25 \pm 5$ kJ/mol. This measured E_a value compares well with the reported value for the energy associated with the breaking of an ice-like hydrogen bond of ∼23 kJ/mol.[2,33−35] Additionally, it agrees with the energy value from a study of the dielectric properties of HCl-doped ice by Takei and Maeno.[36] In their model, an HCl molecule is considered to replace an H_2O in the ice lattice, generating a Bjerrum *L*-defect and an H_3O^+ ion (i.e. extrinsic protonic defect). The temperature dependence of the ac (or high-frequency) and dc conductivity was measured. The energy of activation for the ac conductivity was attributed to the liberation and migration of *L*-defects. Their reported value is $E_a = 25.0 \pm 0.3$ kJ/mol. The agreement with the present value suggests a common mechanism. For this study, the addition of HCl into the ice films increases the number of protonic and Bjerrum *L*-defects.[2] One proposed mechanism for diffusion of water molecules in ice includes the combined migration of interstitials with *L*-defects.[1,2] If, under the present experimental conditions, the diffusion is mostly limited by *L*-defect migration, then the

TABLE 1: Recent Results for Diffusion in Low-Temperature Ice Films

measuremnt	T_{range} (K)	E_a (kJ/mol)	$10^{18}D$(140 K) (cm^2/s)	ref (year)
$H_2{}^{18}O$ diffusion into crystalline H_2O ice	155−165	69.9	0.8	S. M. George[10] (1996)
HDO diffusion into crystalline H_2O or D_2O ice (HDO from isotopic mixture)	153−170	71.1	1.2	S. M. George[11,12,24] (1997, 1998, 1999)
HDO diffusion into crystalline D_2O ice (HDO from H/D exchange of HCl on D_2O ice surface)	146−161	79.5	5.2	S. M. George[24] (1999)
HDO diffusion into D_2O crystalline ice (HDO from H/D exchange of HNO_3 on ice surface)	146−161	55.2	0.2	S. M. George[24] (1999)
D_2O diffusion into surface (ca. 1−5 BL) of amorphous H_2O ice	100−140	13.7	80	H. Kang[13] (2004)
HDO diffusion into HCl-doped crystalline H_2O ice film (HDO from isotopic mixture)	135−145	25	11	this work (2006)

mechanism is similar to the ac conductivity measurements by Takei and Maeno, thereby yielding a similar activation energy.

Discussion

In the discussion that follows, the present results are compared with the results from the previous ice film studies and discussed in terms of a molecular self-diffusion mechanism. Then, the differences between the film studies and the previous bulk ice studies are discussed. Finally, the present results are discussed in terms of an alternative mechanism, namely, a long-range H/D diffusion mechanism by a proton hop−orientational turn sequence.

Comparison of Ice Film Studies. George's research group[10−12] had previously studied diffusion of water in low-temperature ice films. In particular, the diffusion of $H_2{}^{18}O$ and HDO into H_2O ice from 146 to 170 K was examined using a laser-induced thermal desorption technique with mass spectrometric detection. The ice samples were multilayer ice films grown epitaxially on a Ru(001) metal substrate to thicknesses of ∼25−200 BL and were reported to be crystalline according to LEED measurements.[10] After deposition of a thin ice film, a tracer molecule was adsorbed onto the surface. Experiments included $H_2{}^{18}O$ (ca. 1 BL) diffusing into H_2O ice and HDO (ca. 2−9 BL) diffusing into H_2O or D_2O ice. The HDO was produced on the ice surface by the rapid H/D isotopic exchange of D_2O on H_2O ice (or H_2O on D_2O ice). The HDO production and thickness were essentially the same as the present experiments (cf. 2−9 BL to 4−10 BL). Diffusion of the tracer molecule from the surface into the thin ice film was detected by isothermally desorbing the ice multilayer with a laser pulse and then monitoring the water species with mass spectrometry. Diffusion was measured throughout the entire crystalline ice film. An experiment involving 1 BL of $H_2{}^{18}O$ sandwiched between two H_2O ice layers was also performed and yielded similar results. A summary of these results is provided in Table 1. Over the temperature range 146−170 K, the reported energy of activation for self-diffusion of water into crystalline ice films is between 69.9 and 71.1 kJ/mol.[10−12] These values are close to the energy values from the earlier tracer experiments and might suggest a similar mechanism, namely, molecular self-diffusion by interstitials.

George's group also examined the diffusion of HDO diffusing into acid-dosed crystalline D_2O ice films.[32] In these experiments, the HDO was produced by the reaction of HCl or HNO_3 dosed onto the D_2O ice surface. The surface coverage of the acid was 0.3−5 BL for HCl and 0.5−3 BL for HNO_3. The derived diffusion coefficients were independent of acid surface coverage. Relative to the pure ice studies, the HCl-dosed ice films gave increased HDO diffusion, while the HNO_3-dosed ice films gave decreased diffusion (see Table 1). The presence of HCl appears to increase E_a while HNO_3 decreases it. Puzzling, the diffusion coefficients show just the opposite trend for these acid-dosed ices. This group suggested that a compensation effect relates E_a and the diffusion coefficient. It was further suggested that HCl enhances diffusion by creating ionic and Bjerrum *L*-defects while HNO_3 reduces diffusion by forming stable HNO_3−hyrate cages that limit HDO migration.[32]

Kang's research group[13] examined vertical water diffusion into very thin ice films using Cs^+ reactive ion scattering (RIS) with mass spectrometric detection. Amorphous H_2O ice films were vapor-deposited on Ru(0001) between 100 and 140 K with thicknesses of 1−5 BL. A fractional coverage of D_2O was then added onto the ice film. Self-diffusion of D_2O into the H_2O ice film and reverse migration of H_2O to the surface resulted in a change in the surface concentration of the isotopic species, which was detected with a depth resolution of 1 BL. Diffusion into just the top 3 BL was probed. The diffusion followed first-order kinetics, yielding a first-order rate constant. The rate constant showed Arrhenius-like temperature dependence, yielding an energy of activation of 13.7 kJ/mol. While this energy of activation is rather low, it is very important to note that changes right at the ice surface were probed and the ice sample was amorphous and not crystalline. Interestingly, the activation energy is similar to the energy associated with the motion of interstitials. Hondoh's group[5−7] determined that the energy of activation of interstitials in ice is composed of two components, the energy for interstitial formation and the energy for interstitial motion; i.e., $E_a = E_{if} + E_{im}$. If the energy for interstitial formation is very low, ca. $E_{if} \approx 0$, for the amorphous ice surface due to molecular disorder and high defect concentrations, then $E_a \approx E_{im}$, where $E_{im} = 15.4$ kJ/mol. Thus, the close agreement between Kang's E_a and Hondoh's E_{im} suggests that the measured diffusion is due to an interstitial mechanism. Finally, a diffusion coefficient at 140 K was estimated using the diffusion equation, $\langle x^2 \rangle = 2Dt$, equating the first-order half-life with the diffusion time and assuming that the diffusion length for was one interlayer spacing (ca. 1 BL = 0.366 nm). This produced $D(140\ \text{K}) = 8 \times 10^{-17}\ \text{cm}^2/\text{s}$.

For the present experiments, a few bilayers of D_2O were vapor-deposited on a pure crystalline H_2O ice film or an HCl-doped ice film. Upon deposition, H/D isotopic exchange quickly converted the D_2O layer into an HDO-rich mixture layer. Infrared absorption spectroscopy was used to follow the changes of the HDO from the initial HDO mixture layer to HDO isolated in the H_2O ice film. The absorbance of isolated HDO displayed first-order kinetics on acid-doped ice films and was attributed to diffusion of HDO. An Arrhenius analysis produced an activation energy of 25 ± 5 kJ/mol.

A diffusion coefficient can be estimated, similar to Kang's study as presented above,[13] using the measured first-order rate constant, an assumed diffusion length, and the one-dimensional Einstein−Smoluchowski diffusion equation, $\langle x^2 \rangle = 2Dt$. The

diffusion time was equated to the first-order half-life at 140 K (ca. the midrange temperature): $k = 7.2 \times 10^{-4}$ s^{-1} and the half-life is 960 s (or 16 min). Therefore, a diffusion time of $t =$ 16 min was assumed. Since the initial HDO mixture layer was 4−10 BL thick, it was assumed that the HDO would have to diffuse a *typical* length of about 4 BL (ca. 1.464 nm) from the HDO-rich mixture layer into the ice film. Using these values for t and x in the one-dimensional diffusion equation, gives an estimated diffusion coefficient of $D(140\ \text{K}) = 1.1 \times 10^{-17}$ cm^2/s. This value is obviously an estimate that is highly dependent upon the stated approximations. For comparative purposes, the diffusion coefficient at 140 K was calculated for the other ice film studies using the published diffusion data. A summary of the results are presented in Table 1.

In a comparison of the film results, the activation energy varies from 13.7 to 79.5 kJ/mol while the diffusion coefficient at 140 K varies from $(0.2-80) \times 10^{-18}$ cm^2/s. In an explanation of these differences, there are at least two important aspects to keep in mind: (1) the ice morphology (i.e. amorphous, polycrystalline, or crystalline ice); (2) the depth probed (i.e. surface, subsurface, or interior ice). George's ice films were thought to be single crystals with fairly few defects. Diffusion was probed through the entire thickness of the ice film (ca. 25−200 BL). The E_a values are large and very similar to those reported for diffusion in bulk ice. The calculated diffusion coefficients represent the smallest values. Kang's ice films were amorphous and presumably had many structural defects. Diffusion was probed at the surface to a depth of ∼3 BL. This study yielded the lowest E_a and the largest diffusion coefficient. The present ice films were thought to be mostly polycrystalline and therefore possessed more defects than single-crystal ice but less than amorphous ice. Furthermore, the addition of HCl increases the number of defects. Diffusion was probed across the interface between the HDO mixture layer and the underlying acid-doped ice film, ∼4−10 BL below the ice surface. The E_a and diffusion coefficient values are intermediate between the other studies. Thus, the results agree with expectations on the basis of the ice morphology and the experimental depth probed by the different techniques.

Comparison to Bulk Ice Studies. To compare these recent ice film studies to the previous bulk ice studies, the bulk ice results are first summarized.[1] These studies were performed at modestly low temperatures between ∼238 and 271 K and used the isotopic probes $H_2{}^{18}O$, D_2O, and T_2O as tracers to follow the diffusion process. Bulk ice samples of polycrystalline ice, artificially grown single-crystal ice, and naturally grown single-crystal ice, including diffusion for different crystallographic orientations, were examined. Microtome sectioning of the bulk ice (ca. 1 cm thick) into very thin layers (ca. 5 μm) followed by scintillation or mass spectrometric detection was used to measure the diffusion of the tracer species. Over the temperature range studied, the diffusion coefficient fits the standard Arrhenius expression, $D = D_0\, e^{-E_a/RT}$, with the following range of values: $D_0 = 0.6-330$ cm^2/s and $E_a = 52.1-65.6$ kJ/mol. Hobbs summaries the data from all the tracer experiments as $D(263\ \text{K}) \sim 2 \times 10^{-11}$ cm^2/s and $E_a \sim 62.7$ kJ/mol;[1] the study by Ramseier gave the typical results of $D(263\ \text{K}) = 1.49 \times 10^{-11}$ cm^2/s and $E_a = 59.8$ kJ/mol[3], and the interstitial study by Hondoh's group gave $D(263\ \text{K}) \approx 2 \times 10^{-11}$ cm^2/s and $E_a = 54.0$ kJ/mol.[5−7] From these values, the diffusion coefficient was estimated by extrapolation to the midrange temperature of 140 K to be $D(140\ \text{K}) \sim 2 \times 10^{-22}$, 6×10^{-22}, and 1×10^{-22} cm^2/s, respectively, or simply an average value of $D(140\ \text{K}) \sim 3 \times 10^{-22}$ cm^2/s. Comparison of this average diffusion coefficient at 140 K from the higher temperature bulk ice studies to those in Table 1 for the low-temperature ice films indicates a large discrepancy of 10^3 times and more.

At least three possible explanations have been presented in the literature for the large difference in the diffusion coefficients and activation energies between the previous, higher temperature bulk ice studies and the more recent, low-temperature ice film studies. The first and simplest explanation is that the extrapolation of Arrhenius-like behavior is not valid from ∼250 K to the lower temperatures.[10] Small uncertainties in the preexponential factor and the energy term are greatly magnified when the extrapolation is as great as 100 K. Thus, it is simply inappropriate to expect the diffusion results from the two types of studies to overlap.

The second explanation is that the mechanism for molecular self-diffusion in ice changes between the two temperature ranges. The mechanism involves migration of lattice defects, either interstitials or vacancies, where interstitials are H_2O molecules in ice that do not occupy regular crystal lattice sites, while vacancies are unoccupied crystal lattice sites. Migration by these molecular defects may also be assisted by ionic and Bjerrum defects.[1,2] The research by Hondoh's group[5−7] appears to confirm that the major mechanism involves migration by interstitials for $T \geq 220$ K. For this mechanism, the diffusion depends on the number or concentration of interstitials in ice. For the lower temperatures, the concentration of interstitials may become vanishingly small. Thus, George's group has suggested that the mechanism may involve migration by vacancies at the lower temperature range.[37] Recent work from this group concerning diffusion of other small molecules in ice films appears to suggest a vacancy mechanism.[37]

The third explanation concerns the structure or morphology of vapor-deposited, low-temperature ice films. Microstructures in ice films including increased defects, dislocations, and grain boundaries may increase diffusion relative to diffusion in bulk ice samples.[1,2,27,30] For example, assuming that the mechanism involves interstitials and the diffusion coefficient is proportional to the concentration of interstitials, then the increased diffusion coefficient at low temperature may reflect an increase in the concentration of interstitial defects for the vapor-deposited ice films. George's group previously suggested that since the very thin ice films have a large surface-to-volume ratio, the concentration of interstitials in the ice multilayers may be increased due to perturbations of the nearby surface.[10] Alternatively, if the low-temperature ice films are polycrystalline rather than single crystals, these ice films will have an increased number of defects, dislocations, and grain boundaries. Self-diffusion along these ice defects may be enhanced relative to the higher-temperature, bulk ices. This would be especially true for the acid-doped ice films, where clusters of acid hydrates may increase the number of defects.[27] Finally, and unique to vapor-deposited ice films, cubic crystalline ice (I_c between 130 and 150 K), hexagonal crystalline ice (I_h for $T > 150$ K), or a mixture can be formed depending upon the temperature and deposition procedure.[2] A mixture would have an increased number of structural defects that might increase diffusion.

Presently, it is suggested that differences in the ice morphology are probably responsible for the differences in the results for diffusion of water in vapor-deposited ice films and bulk crystalline ice. As discussed above, the results for the film studies appear to be dependent upon the morphology, whether amorphous, polycrystalline, or crystalline, and the depth of diffusion probed, whether surface, subsurface, or interior ice. Structural defects must play an important role. Vapor-deposited

films, controlled by condensation kinetics, have more defects than bulk ice samples that have been carefully prepared under equilibrium conditions by freezing water. Films have a larger surface-to-volume ratio, and the surface may induce more defects deeper into the films compared to bulk ice samples. Finally, the diffusion depth probed for the ice film studies varied from 1 to ~100 nm, while the bulk ice studies probed interior ice on the order of 1 cm thick.

Long-Range H/D Diffusion Mechanism. Finally, an alternative explanation for the present spectroscopic results involves long-range H/D diffusion rather than a molecular self-diffusion mechanism. This diffusion mechanism is effectively the same as the H/D isotopic exchange mechanism proposed and developed by Devlin and co-workers.[2,19,20] They have successfully applied this mechanism to the observed H/D exchange in pure bulk ice and both pure and HCl-doped ice nanocrystals. According to this mechanism, the first step involves the passage of a protonic defect through adjacent H_2O and D_2O molecules in the ice lattice to form the nearest-neighbor group $(HDO)_2$. The second step involves the passage of an orientational Bjerrum *L*-defect. This defect flips the orientation of the HDO molecules in the $(HDO)_2$ species to form two *isolated* HDO molecules separated by two oxygen atoms. For the present results, the $(HDO)_2$ species already exists in the isotopic mixture layer, due to the initial rapid H/D exchange of D_2O on the ice film, as shown in Figure 2a. It is the formation of isolated HDO by step 2 above that could involve long-range, multiple passage of a protonic defect followed by the passage of an orientational Bjerrum *L*-defect. Thus, a series of multiple proton hopping and orientational turning steps could move D toward the interior and H toward the surface, leading to isotopic mixing and the formation of *isolated* HDO molecules. This long-range H/D diffusion is highly unlikely in pure ice films because of slow proton hopping over the estimated distance (ca. 4 BL), which is consistent with the present results for diffusion on pure ice films. However, for the acid-doped ice films, the increased proton activity could increase the proton hopping step, such that a series of multiple hopping followed by orientational turn steps could cause the observed H/D diffusion. Concerning the "off−on" behavior with acid concentration, once the acid reaches a certain activity level that turns on the H/D diffusion, the diffusion would then be limited by the turn step. Thus, additional acid would not necessarily cause the diffusion to be faster but would be limited by the rate of the orientational turn step. This alternative H/D diffusion mechanism therefore appears to account for the present results. Additionally, this mechanism is consistent with the very recent work from Kang's group,[31] as pointed out in the Results. For these reasons, it is the favored mechanism for explaining the present results.

Conclusion

In this study, infrared absorption spectroscopy was used to follow the changes of HDO from an initial HDO mixture layer on an ice film to HDO isolated in the ice. This was possible because isolated HDO in H_2O ice has a unique spectrum that can be distinguished from the spectrum of the HDO mixture layer. The absorbance of isolated HDO displayed first-order kinetics and was attributed to diffusion of HDO in the H_2O ice film. While negligible diffusion was observed for pure ice films and for ice films with low HCl concentrations, diffusion of HDO occurred for higher HCl concentrations with a concentration-independent rate constant. The diffusion under these conditions followed Arrhenius behavior yielding $E_a = 25 \pm 5$ kJ/mol. These new results and analysis correct an earlier study[15] in which the spectral changes were attributed to H/D isotopic exchange on H_2O ice.

These spectroscopic results compare favorably with recent studies of diffusion in low-temperature ice films.[10−14] The present activation energy falls between the values for diffusion in crystalline ice films and amorphous ice films, while the estimated diffusion coefficient at 140 K is very similar to the value from a study of HDO diffusion in HCl-dosed ice films.[30] However, the results from all the ice film studies at low temperatures differ from earlier bulk ice studies at higher temperatures. In particular, extrapolation of the results from the bulk ice studies to 140 K yields an estimated diffusion coefficient that is at least 10^3 times smaller than the values determined from the ice film studies. The discrepancy is probably due to differences in the ice structure or morphology between vapor-deposited ice films and bulk ice samples. Microstructures in ice films including increased defects, dislocations, and grain boundaries would increase diffusion relative to diffusion in bulk crystalline ice samples.

Furthermore, in comparing studies, it is important to note that HDO can diffuse in ice by two mechanisms: (1) self-diffusion by either interstitial or vacancy migration; (2) H/D diffusion by a series of proton hop−molecular orientational turn steps. In "neutral" ice, the self-diffusion mechanism operates and is slow. Again, on the basis of the bulk ice studies, it is therefore surprising that self-diffusion in low-temperature films has been observed. For acid-doped ice, the excess protons turn on the long-range hop−turn mechanism, thereby enhancing HDO diffusion in low-temperature ice films.

Acknowledgment. This research has greatly benefited from many helpful and insightful discussions with Professor Devlin. We gratefully acknowledge the financial support of the Welch Foundation and the Dreyfus Foundation.

References and Notes

(1) Hobbs, P. V. *Ice Physics*; Clarendon Press: Oxford, U.K., 1974.
(2) Petrenko, V. F.; Whitworth, R. W. *Physics of Ice*; Oxford University Press: New York, 1999.
(3) Ramseier, R. O. *J. Appl. Phys.* **1967**, *38*, 2553.
(4) Onsager, L.; Runnels, L. K. *J. Chem. Phys.* **1969**, *50*, 1089.
(5) Hondoh, T.; Itoh, T.; Higashi, A. *Jpn. J. Appl. Phys.* **1981**, *20*, 737.
(6) Hondoh, T.; Itoh, T.; Amakai, S.; Goto, K.; Higashi, A. *J. Phys. Chem.* **1983**, *87*, 4040.
(7) Goto, K.; Hondoh, T.; Higashi, A. *Jpn. J. Appl. Phys.* **1986**, *25*, 351.
(8) Itoh, H.; Kawamura, K.; Hondoh, T.; Mae, S. *J. Chem. Phys.* **1996**, *105*, 2408.
(9) Ikeda-Fukazawa, T.; Horikawa, S.; Hondoh, T.; Kawamura, K. *J. Chem. Phys.* **2002**, *117*, 3886.
(10) Brown, D. E.; George, S. M. *J. Phys. Chem.* **1996**, *100*, 15460.
(11) Livingston, F. E.; Whipple, G. C.; George, S. M. *J. Phys. Chem. B* **1997**, *101*, 6127.
(12) Livingston, F. E.; Whipple, G. C.; George, S. M. *J. Chem. Phys.* **1998**, *108*, 2197.
(13) Jung, K.-H.; Park, S.-C.; Kim, J.-H.; Kang, H. *J. Chem. Phys.* **2004**, *121*, 2758.
(14) Park, S.-C.; Jung, K.-H.; Kang, H. *J. Chem. Phys.* **2004**, *121*, 2765.
(15) Everest, M. A.; Pursell, C. J. *J. Chem. Phys.* **2001**, *115*, 9843.
(16) Holt, J. S.; Sadoskas, D.; Pursell, C. J. *J. Chem. Phys.* **2004**, *120*, 715343.
(17) Zeisberg, F. C.; van Arsdel, W. B.; Blake, F. C.; Greenwalt, C. H.; Taylor, G. B. In *International Critical Tables*; Washburn, E. W., West, C. J., Dorsey, N. E., Eds.; McGraw-Hill: New York, 1926; Vol. 3, pp 301.
(18) Tolbert, M. A.; Middlebrook, A. M. *J. Geophys. Res. Atmos.* **1990**, *95*, 22423.
(19) Devlin, J. P. *Int. Rev. Phys. Chem.* **1990**, *9*, 29 and references therein.
(20) Uras-Aytemiz, N.; Joyce, C.; Devlin, J. P. *J. Chem. Phys.* **2001**, *115*, 9835.

(21) Haas, C.; Hornig, D. F. *J. Chem. Phys.* **1960**, *32*, 1763.
(22) Devlin, J. P.; Wooldridge, P. J.; Ritzhaupt, G. *J. Chem. Phys.* **1986**, *84*, 6095.
(23) Haynes, D. R.; Tro, N. J.; George, S. M. *J. Phys. Chem.* **1992**, *96*, 8502.
(24) Livingston, F. E.; George, S. M. *J. Phys. Chem. A* **1998**, *102*, 10280.
(25) Smith, J. A.; Livingston, F. E.; George, S. M. *J. Phys. Chem. B* **2003**, *107*, 3871.
(26) Bolton, K.; Pettersson, J. B. C. *J. Phys. Chem. B* **2000**, *104*, 1590.
(27) Thibert, E.; Dominé, F. *J. Phys. Chem. B* **1997**, *101*, 3554.
(28) Haq, S.; Harnett, J.; Hodgson, A. *J. Phys. Chem. B* **2002**, *106*, 3950.
(29) Pursell, C. J.; Zaidi, M.; Thompson, A.; Fraser-Gaston, C.; Vela, E. *J. Phys. Chem. A* **2000**, *104*, 552.
(30) Sadtchenko, V.; Giese, C. F.; Gentry, W. R. *J. Phys. Chem. B* **2000**, *104*, 9421.
(31) Lee, C.-W.; Lee, P.-R.; Kang, H. *Angew. Chem., Int. Ed.* **2006**, *45*, in press.
(32) Livingston, F. E.; George, S. M. *J. Phys. Chem. B* **1999**, *103*, 4366.
(33) Stillinger, F. *Science* **1980**, *209*, 451.
(34) Suresh, S. J.; Naik, V. M. *J. Chem. Phys.* **2000**, *113*, 9727−9732.
(35) Smith, J. D.; Cappa, C. D.; Wilson, K. R.; Messer, B. M.; Cohen, R. C.; Saykally, R. J. *Science* **2004**, *306*, 851−853.
(36) Takei, I.; Maeno, N. *J. Chem. Phys.* **1984**, *81*, 6186.
(37) Livingston, F. E.; Smith, J. A.; George, S. M. *J. Phys. Chem. A* **2002**, *106*, 6309.